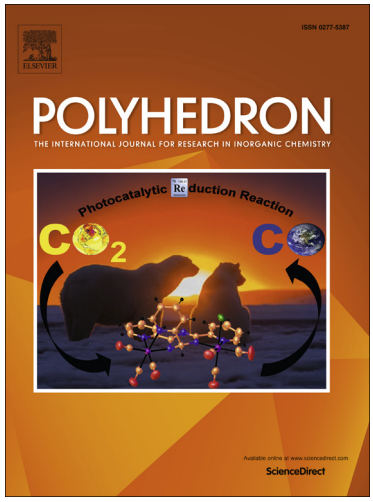

Aluminum Methyl and Isopropoxide Complexes with Ketiminate Ligands: Synthesis, Structural Characterization and Ring-Opening Polymerization of Cyclic Esters

Cigdem Tuc Altaf, Haobing Wang, Maryam Keram, Yang Yang, Haiyan Ma

PII: S0277-5387(14)00372-6
DOI: http://dx.doi.org/10.1016/j.poly.2014.05.055
Reference: POLY 10770

To appear in: *Polyhedron*

Received Date: 25 March 2014
Accepted Date: 22 May 2014

Please cite this article as: C.T. Altaf, H. Wang, M. Keram, Y. Yang, H. Ma, Aluminum Methyl and Isopropoxide Complexes with Ketiminate Ligands: Synthesis, Structural Characterization and Ring-Opening Polymerization of Cyclic Esters, *Polyhedron* (2014), doi: http://dx.doi.org/10.1016/j.poly.2014.05.055

Aluminum Methyl and Isopropoxide Complexes with Ketiminate Ligands: Synthesis, Structural Characterization and Ring-Opening Polymerization of Cyclic Esters

Cigdem Tuc Altaf, Haobing Wang, Maryam Keram, Yang Yang, Haiyan Ma[a,*]

Shanghai Key Laboratory of Functional Materials Chemistry and Laboratory of Organometallic Chemistry, East China University of Science and Technology, 130 Meilong Road, Shanghai, 200237, P. R. China.

* Corresponding author. Tel/Fax:: +86-21-64253519; EM: haiyanma@ecust.edu.cn

Submitted to Polyhedron

Revised and re-submitted in

Revised and re-submitted in

Abstract

Mono(ketiminate) aluminum dimethyl complexes **1a-5a** and bis(ketiminate) aluminum methyl complex **2b** were synthesized via the reactions of $AlMe_3$ with various *N*-aryl substituted ketimine compounds in a 1:1 or 1:2 molar ratio, respectively. The reaction of $Al(O^iPr)_3$ with the ketimine compound $\mathbf{L^2H}$ resulted in a bis(ketiminate) aluminum isopropoxide complex **2c**. All the complexes were characterized by ^1H and $^{13}C\{^1H\}$ NMR spectroscopy, either EA or HRMS analysis. *X*-ray diffraction measurement of complexes **2a** and **3a** confirmed that in the solid state both **2a** and **3a** exist as a tetrahedron structure with the aluminum atom center surrounded by the oxygen and nitrogen donors of the bis-chelating ketiminate ligand as well as two methyl groups. Besides, a triligated aluminum complex **3** ($Al(L^3)_3$) with a six-coordinated metal core and a dinuclear aluminum isopropoxide complex **6d** $[(L^6)_2Al(\mu\text{-}O^iPr)_2Al(O^iPr)_2]$ with C_2-symmetry were isolated and characterized by *X*-ray diffraction studies. All aluminum methyl complexes behaved as active initiators in the ring-opening polymerization (ROP) of *rac*-lactide (*rac*-LA), affording isotactic-enriched polylactides (PLAs) with high molecular weights and broad molecular weight distributions at 70 °C. The steric and electronic characters of the ancillary ligands show significant effects both on the activity and the stereoselectivity. The introduction of an electron-withdrawing group on the *para*-position of *N*-aryl ring of the ligand resulted in an increase of the catalytic activity. However, the electronic character of ancillary ligands showed a neglectable effect on the ROP of ε-CL initiated by these aluminum complexes. For both monomers, bis(ketiminate) aluminum complex **2b** was found to be more active than the corresponding mono(ketiminate) complex **2a** of the same ligand. Aluminum isopropoxide complex **2c** exerted better control for the polymerizations of both monomers, providing polymers with narrower

molecular weight distributions and smaller molecular weights which are comparable to the theoretical values.

Keywords: aluminum, ketiminate ligand, catalyst, cyclic ester, ring-opening polymerization

1. Introduction

Polylactides (PLAs) and related polyesters have gained great attention in the past decades for wide applications in medical and pharmaceutical fields due to their biodegradable, biocompatible, and permeable properties [1-8]. Nowadays, polylactides are further considered to be ideal alternatives for commercial olefinic polymers regarding the fact that they are produced from completely renewable resources in addition to possessing excellent physical/mechanical properties. Catalytic ring-opening polymerization (ROP) of related cyclic esters is the major method adopted to synthesize these polymers [9-12]. During the polymerization process, higher activities and better control can be expected in due course by further optimizing the initiator structure.

Studies have shown that numerous aluminum complexes display good catalytic performance toward the ring-opening polymerization of lactide (LA) or ε-caprolactone (ε-CL), most of them are aluminum alkyl [13-23] and alkoxide complexes [24-43] supported by multidentate ancillary ligands. As expected, the surrounding coordinated ancillary ligands affect both the stability of the complexes and their catalytic performance in the ROP of cyclic esters. Among them, aluminum complexes based on salen [24, 25, 34-36, 38-48], salan [49, 50], or related $\{ONNO\}^{2-}$ [50-52], $\{ONO\}^{2-}$ [21,54] ligand frameworks are the most attractive, since they are capable of producing highly isotactic polylactides from racemic lactide monomers, which are of high interest due to the enhanced thermal and mechanical properties by forming stereocomplexes [55].

Due to the versatile modification possibilities of the ligand framework, aluminum complexes of β-diketiminate ligands and analogues belong to another widely studied branch [56-60]. Our previous work showed that aluminum ethyl complexes bearing β-diketiminate ligands with bulky *N*-aryl substituents could initiate the ROP of ε-CL with moderate activities, affording

polycaprolactones with broad molecular weight distributions [56]. Recently, Peng and coworkers reported that aluminum alkyl complexes bearing aliphatic *N*-substituted *β*-diketiminate ligands also showed activities toward the polymerization of *ε*-CL in the absence of alcohol [60]. Unfortunately, none of these *β*-diketiminate aluminum complexes are active for the ROP of *rac*-lactide (*rac*-LA). The steric bulkiness of *β*-diketimine ligand is suggested to be disadvantageous in the polymerization of *rac*-LA because that it may significantly hinder the coordination/insertion of lactide monomer to the metal center. Previously, Huang and coworkers [14] found that aluminum complexes with a less steric bulky ketiminate ligand {κ^2-OCMeCHCMeN-(2,6-^{i}Pr$_2$C$_6$H$_4$)}AlR$_2$ (R = Me, Et, Cl) could initiate the ring-opening polymerization of ε-CL at room temperature and 60 °C to yield high molecular weight PCLs with broad PDIs (1.29–2.80). However, the study did not include the electronic and steric effect of ketiminate ligands on the polymerization as well as the potential catalysis for the ROP of lactide. In view of the less steric bulkiness in comparison with *β*-diketiminate ligands, ketiminate ligands may serve as a suitable ligand framework to develop active aluminum initiators for the ROP of *rac*-lactide. Therefore, in this work, ketiminate ligands bearing various electron-donating and electron-withdrawing groups were used to synthesize aluminum ketiminate complexes, which were further evaluated for the ROP of *rac*-LA and ε-CL monomers.

2. Experimental

2.1. General methods

All manipulations were carried out under a dry argon atmosphere using standard Schlenk techniques and a glove box unless otherwise indicated. Toluene, *n*-hexane, light petroleum ether were refluxed over sodium-benzophenone prior to use. Chloroform-*d* was dried over calcium hydride. Corresponding ketimine compounds, 2-(*N*-2,6-dimethylphenyl)aminopent-2-en-4-one (**L^{1}H**), 2-(*N*-2,6-dichlorophenyl)aminopent-2-en-4-one (**L^{2}H**), 2-(*N*-4-tertbutylphenyl)aminopent-2-en-4-one (**L^{3}H**), 2-(*N*-4-methoxyphenyl)aminopent-2-en-4-one (**L^{4}H**), 2-(*N*-4-chlorophenyl)aminopent-2-en-4-one (**L^{5}H**), 2-(*N*-4-triflouromethylphenyl)aminopent-2-en-4-one (**L^{6}H**) were prepared according to the previously published procedure [56]. NMR spectra were recorded on a Bruker AVANCE-400 spectrometer with $CDCl_3$ as solvent (^{1}H: 400 MHz; ^{13}C {^{1}H}: 101 MHz). Chemical shifts for ^{1}H and ^{13}C {H} NMR spectra were referenced internally using the residual solvent resonances and reported relative to tetramethylsilane (TMS). Elemental analyses were performed on an EA-1106 instrument. Gel permeation chromatography (GPC) analyses were carried out on a Waters instrument (M515 pump, Optilab Rex injector) in THF at 25 °C, at a flow rate of 1 mL·min^{-1}. Calibration standards were commercially available narrowly distributed linear polystyrene samples that cover a broad range of molar masses (10^3 < M < 2×10^6 g· mol^{-1}).

2.2. Synthesis of aluminum complexes

*2.2.1. Synthesis of N-(2,6-dimethylphenyl)ketiminate aluminum dimethyl complex (κ^2-OCMeCHCMeN-2,6-$Me_2C_6H_3$)$AlMe_2$ (**1a**)*

$AlMe_3$ (1.2 mL, 2.0 M, 2.3 mmol) was added to a toluene solution (20 mL) of **L^{1}H** (0.406 g, 2.30 mmol) at 0 °C in a glove box. The mixture was then allowed to warm to room temperature

and stirred for additional 3 h. The resulting mixture was dried under vacuum to yield a pale yellow oily product. Recrystallization with toluene at −20 °C resulted in colorless crystalline solids (0.300 g, 51%). ^{1}H NMR (400 MHz, $CDCl_3$, 25 °C): δ 7.08 (m, 3H, *m*, *p-H* of Ar), 5.28 (s, 1H, CMeC*H*CMe), 2.12 (s, 6H, Ar-CH_3), 2.07 (s, 3H, CH_3), 1.67 (s, 3H, CH_3), −0.91 (s, 6H, Al-CH_3). ^{13}C{H} NMR (100 MHz, $CDCl_3$, 25 °C): δ 181.3 (*C*=O), 175.5 (*C*-N), 141.7 (Ar-*C*), 132.3 (Ar-*C*), 128.7 (Ar-*C*), 126.3 (Ar-*C*), 99.6 (*C*H), 25.8 (*C*H_3), 22.2 (*C*H_3), 18.3 (*C*H_3), −10.2 (Al-*C*H_3). Anal. Calcd. for $C_{15}H_{22}AlNO$: C, 69.47; H, 8.55; N, 5.40. Found: C, 68.74; H, 8.45; N, 5.11%. Calcd. HRMS for $C_{15}H_{22}AlNO$: 259.1517; found: 259.1514. m/z (%): 258.1413 [trace, M^+], 244.1246 [100, M − CH_3^+], 188.1066 [2.2, 2,6-$CH_3C_6H_3N$=$C(CH_3)OC(CH_3)$ − CH_3^+].

*2.2.2. Synthesis of N-(2,6-dichlorolphenyl)ketiminate aluminum dimethyl complex (κ²-OCMeCHCMeN-2,6-$Cl_2C_6H_3$)$AlMe_2$ (**2a**)*

Similar reaction route as that of **1a** was adopted. $AlMe_3$ (2.0 mL, 2.0 M, 4.0 mmol) was added to a stirred toluene solution of **L²H** (0.980 g, 4.00 mmol) at 0 °C in a glove box. Recrystallization of the crude product with a mixture of toluene and hexane resulted in colorless crystals (0.780 g, 65%). ^{1}H NMR (400 MHz, $CDCl_3$, 25 °C): δ 7.39 (d, 2H, *J* = 8.0 Hz, *m-H* of Ar), 7.16 (t, 1H, *J* = 8.0 Hz, *p-H* of Ar), 5.36 (s, 1H, CMeC*H*CMe), 2.11 (s, 3H, CH_3), 1.77 (s, 3H, CH_3), −0.87 (s, 6H, Al-CH_3). ^{13}C{H} NMR (100 MHz, $CDCl_3$, 25 °C): δ 183.3 (*C*=O), 175.5 (*C*-N), 138.5 (Ar-*C*), 130.8 (Ar-*C*), 127.9 (Ar-*C*), 126.9 (Ar-*C*), 99.0 (*C*H), 25.1 (*C*H_3), 21.7 (*C*H_3), −11.1 (Al-*C*H_3). Anal. Calcd. for $C_{13}H_{16}AlCl_2NO$: C, 52.02; H, 5.37; N, 4.67. Found: C, 51.80; H, 5.17; N, 4.86%.

*2.2.3. Synthesis of N-(p-isopropylphenyl)ketiminate aluminum dimethyl complex (κ²-OCMeCHCMeN-p-$CH(CH_3)_2C_6H_4$)$AlMe_2$ (**3a**)*

$AlMe_3$ (2.0 mL, 2.0 M, 4.0 mmol) was added to a toluene solution (20 mL) of **L^3H** (0.870 g, 4.00 mmol) at 0 °C in a glove box. The mixture was then allowed to warm to room temperature and stirred overnight. The mixture was vacuum-dried to yield a yellow oily product. Recrystallization of the crude product with a mixture of toluene and hexane resulted in colorless crystals (0.480 g, 44%). ^{1}H NMR (400 MHz, $CDCl_3$, 25 °C): δ 7.20 (d, 2H, *J* = 8.0 Hz, o-*H* of Ar), 6.85 (d, 2H, *J* = 8.0 Hz, m-*H* of Ar), 5.18 (s, 1H, CMeC*H*CMe), 2.91 (septet, *J* = 6.8 Hz, 1H, C*H*$(CH_3)_2$), 2.03 (s, 3H, CH_3), 1.79 (s, 3H, CH_3), 1.26 (d, *J* = 6.8 Hz, 6H, CH(C$H_3)_2$), −0.91 (s, 6H, Al-CH_3). ^{13}C{H} NMR (100 MHz, $CDCl_3$): δ 179.6 (*C*=O), 173.5 (*C*-N), 146.0 (Ar-*C*), 140.5 (Ar-*C*), 126.3 (Ar-*C*), 123.6 (Ar-*C*), 98.5 (*C*H), 32.6 (*C*H$(CH_3)_2$), 24.7 (*C*H_3), 23.0 (*C*H_3), 21.7 (*C*H_3), −11.4 (Al-*C*H_3). Anal. Calcd. for $C_{16}H_{24}AlNO$: C, 70.30; H, 8.85; N, 5.12. Found: C, 69.25; H, 8.89; N, 4.89%. Calcd. HRMS for $C_{16}H_{24}AlNO$: 273.1673; found: 273.1682. m/z (%): 272.2 ($[M-H]^+$, 15.9), 258.2 ($[M-CH_3]^+$, 100), 216.2($[L]^+$, 23.7).

*2.2.4. Synthesis of N-(p-methoxyphenyl)ketiminate aluminum dimethyl complex (κ^2-OCMeCHCMeN-p-$OCH_3C_6H_4$)$AlMe_2$ (**4a**)*

$AlMe_3$ (1.0 mL, 2.0 M, 2.0 mmol) was added to toluene solution of **L^4H** (0.410 g, 2.00 mmol) at 0 °C in a glove box and was stirred overnight. The resulting reaction mixture was dried under vacuum to yield a pale yellow oily product. Recrystallization of the crude product with toluene resulted in colorless crystals (0.280 g, 54%). ^{1}H NMR (400 MHz, $CDCl_3$, 25 °C): δ 6.90 (d, 2H, *J* = 9.3 Hz, o-*H* of Ar), 6.85 (d, 2H, *J* = 9.3 Hz, m-*H* of Ar), 5.17 (s, 1H, CMeC*H*CMe), 3.81 (s, 3H, Ar-OCH_3), 2.03 (s, 3H, CH_3), 1.79 (s, 3H, CH_3), −1.03 (s, 6H, Al(C$H_3)_2$). ^{13}C{H} NMR (100 MHz, $CDCl_3$, 25 °C): δ 179.8 (O=*C*), 173.9 (N-*C*), 157.0 (Ar-*C*), 135.7 (Ar-*C*), 124.8 (Ar-*C*H), 113.6 (Ar-*C*), 98.5 (*C*H), 54.4 (O*C*H_3), 24.8 (*C*H_3), 21.6 (*C*H_3), −11.4 (Al-*C*H_3). Anal. Calcd. for $C_{14}H_{20}AlNO_2$: C, 64.35; H, 7.71; N, 5.36. Found: C, 64.46; H, 7.98; N, 5.10%.

*2.2.5. Synthesis of N-(p-chlorophenyl)ketiminate aluminum dimethyl complex (κ^2-OCMeCHCMeN-p-ClC_6H_4)$AlMe_2$ (**5a**)*

$AlMe_3$ (2.0 mL, 2.0 M, 4.0 mmol) was added to toluene solution of $\mathbf{L^5H}$ (0.839 g, 4.00 mmol) and the reaction mixture was stirred overnight. The reaction mixture was then dried under vacuum to yield a pale yellow oily product. Recrystallization of the crude product with toluene resulted in colorless crystals (0.450 g, 42%). ^{1}H NMR (400 MHz, $CDCl_3$, 25°C): δ 7.35 (d, 2H, *J* = 8.5 Hz, *o-H* of Ar), 6.89 (d, 2H, *J* = 8.5 Hz, *m-H* of Ar), 5.21 (s, 1H, CMeC*H*CMe), 2.04 (s, 3H, CH_3), 1.79 (s, 3H, CH_3), –0.92 (s, 6H, Al-CH_3). ^{13}C{H} NMR (100 MHz, $CDCl_3$, 25°C): δ 180.9 (O=*C*), 173.5 (N-*C*), 141.6 (Ar-*C*), 131.2 (Ar-*C*), 128.6 (Ar-*C*), 125.4 (Ar-*C*), 98.7 (*C*H), 24.8 (*C*H_3), 21.7 (*C*H_3), –11.4 (Al-*C*H_3). Anal. Calcd. for $C_{13}H_{17}AlClNO$: C, 58.76; H, 6.45; N, 5.27. Found: C, 58.30; H, 6.59; N, 5.34%.

*2.2.6. Synthesis of bis{N,-(2,6-dichlorophenyl)ketiminate} aluminum methyl complex (κ^2-OCMeCHCMeN-2,6-$Cl_2C_6H_3$)$_2AlMe$ (**2b**)*

$AlMe_3$ (1.0 mL, 2.0 M, 2.0 mmol) was added to a stirred toluene solution (20 mL) of $\mathbf{L^2H}$ (0.980 g, 4.00 mmol) at 0 °C. The reaction mixture was stirred in an oil bath at 90 °C for 3 days. The resulting reaction mixture was dried under vacuum to yield a pale yellow oily product. Recrystallization of the crude product with toluene resulted in colorless crystalline solids (0.450 g, 42%). ^{1}H NMR (400 MHz, $CDCl_3$, 25 °C): δ 7.33 (dd, 2H, ^4J = 1.3 Hz, ^3J = 8.0 Hz, *m-H* of Ar), 7.29 (dd, 2H, ^4J = 1.3 Hz, ^3J = 8.0 Hz, *m-H* of Ar), 7.03 (t, 2H, *J* = 8.0 Hz, *p-H* of Ar), 5.15 (s, 2H, CMeC*H*CMe), 1.65 (s, 6H, CH_3), 1.35 (s, 6H, CH_3), –0.88 (s, 3H, Al-CH_3). ^{13}C{H} NMR (100 MHz, $CDCl_3$, 25 °C): δ 180.7 (O-*C*), 174.1 (*C*-N), 145.1 (Ar-*C*), 131.1 (Ar-*C*), 130.6 (Ar-*C*), 127.0 (Ar-*C*), 126.6 (Ar-*C*), 124.5 (Ar-*C*), 98.0 (*C*H), 23.7 (*C*H_3), 22.8 (*C*H_3), –8.5 (Al-

197 CH_3). Anal. Calcd. for $C_{23}H_{23}AlCl_4N_2O_2$: C, 52.30; H, 4.39; N, 5.30. Found: C, 52.21; H, 4.24;
198 N, 5.11%.

199 *2.2.7. The reaction of $AlMe_3$ with 2 equiv. of ketimine* ***L^3H***

200 $AlMe_3$ (2 mmol, 1.0 mL, 2.0 M) was added dropwise to a solution of **L^3H** (0.870 g, 4.00
201 mmol) dissolved in 20 mL of toluene. The reaction mixture was stirred in an oil bath at 90 °C
202 for 3 days. The color of the solution turned to reddish brown. The mixture was dried under
203 vacuum to yield a foam-like crude product. White powder could be isolated after recrystallization
204 with light petroleum ether, which was characterized to be complex **3**. ^{1}H NMR (400 MHz,
205 $CDCl_3$, 25 °C): δ 7.23 (d, 1H, *J* = 8.4 Hz, o-*H* of Ar), 7.14-6.98 (m, 5H, *o,m-H* of Ar), 6.90 (d,
206 1H, *J* = 7.2 Hz, *m-H* of Ar), 6.82 (d, 1H, *J* = 8.0 Hz, *m-H* of Ar), 6.73 (d, 1H, *J* = 7.6 Hz, *m-H*
207 of Ar), 6.66 (d, 1H, *J* = 6.8 Hz, o-*H* of Ar), 6.59 (d, 1H, *J* = 6.8 Hz, *m-H* of Ar), 4.99 (s, 1H,
208 CMeC*H*CMe), 4.82 (s, 1H, CMeC*H*CMe), 4.53 (d, 1H, *J* = 7.6 Hz, o-*H* of Ar), 4.37 (s, 1H,
209 CMeC*H*CMe), 2.93 (septet, 1H, *J* = 6.8 Hz, C*H*$(CH_3)_2$), 2.87 (septet, 1H, *J* = 7.2 Hz,
210 C*H*$(CH_3)_2$), 2.75 (septet, 1H, *J* = 6.8 Hz, C*H*$(CH_3)_2$), 1.95 (s, 3H, CH_3), 1.54 (s, 3H, CH_3), 1.52
211 (s, 3H, CH_3), 1.35 (s, 3H, CH_3), 1.32-1.26 (m, 6H, CH(CH_3)$_2$), 1.27 (s, 3H, CH_3), 1.23 (d, 6H, *J*
212 = 6.8 Hz, CH(CH_3)$_2$), 1.21 (s, 3H, CH_3), 1.16 (d, 3H, *J* = 6.8 Hz, CH(CH_3)$_2$), 1.14 (d, 3H, *J* =
213 7.2 Hz, CH(CH_3)$_2$). Anal. Calcd. for $C_{42}H_{54}AlN_3O_3$: C, 74.64; H, 8.05; N, 6.22. Found: C,
214 73.02; H, 7.89; N, 5.36%.

215 *2.2.8. Synthesis of bis[N-(2,6-dichlorophenyl)ketiminate] aluminum isopropoxide complex (*κ^2-
216 *OCMeCHCMeN-2,6-$Cl_2C_6H_3$)$_2$AlOCH$(CH_3)_2$ (**2c**)*

217 A toluene solution of **L^2H** (0.980 g, 4.00 mmol, 20 mL) was mixed with a toluene solution of
218 Al(O^{i}Pr)$_3$ (2.00 mmol, 0.41 g, 0.5 M). The reaction mixture was stirred in an oil bath at 90 °C
219 for 3 days. All the volatiles were removed under vacuum to yield a brown oily product.

Colorless crystals could be isolated after recrystallization with toluene at −20 °C (0.646 g, 67%). ^{1}H NMR (400 MHz, $CDCl_3$, 25 °C): δ 7.36 (d, 2H, *J* = 8.0 Hz, *m*-Ar*H*), 7.29 (d, 2H, *J* = 8.0 Hz, *m*-Ar*H*), 7.05 (t, 2H, *J* = 8.0 Hz, *p*-ArH), 5.21 (s, 4H, γ-C*H*), 3.74 (septet, 2H, *J* = 6.0 Hz, C*H*(CH_3)$_2$), 1.63 (s, 6H, C*H*$_3$), 1.38 (s, 6H, C*H*$_3$), 1.01 (d, 3H, *J* = 6.0 Hz, CH(*CH*$_3$)$_2$), 0.99 (d, 3H, *J* = 6.0 Hz, CH(*CH*$_3$)$_2$). ^{13}C{H} NMR (100 MHz, $CDCl_3$, 25 °C): δ 183.79 (O*C*), 175.93 (N*C*), 145.87 (Ar-*C*), 132.78 (Ar-*C*), 132.19 (Ar-*C*), 128.33 (Ar-*C*), 127.56 (Ar-*C*), 125.94 (Ar-*C*), 99.35 (γ-*C*H), 62.66 (O*C*H(CH_3)$_2$), 27.46 (*C*H$_3$), 27.20 (*C*H$_3$), 24.79 (*C*H$_3$), 24.14 (*C*H$_3$). Anal. Calcd. for $C_{25}H_{27}AlCl_4N_2O_3$: C, 52.47; H, 4.76; N, 4.89. Found: C, 52.62; H, 4.72; N, 4.69%.

2.3. X-ray crystallographic determination

Single crystals suitable for X-ray diffraction studies were obtained from a saturated toluene/hexane mixture for **2a** or **3a**, or a petroleum ether solution for **3**, or a toluene solution for **6d** respectively. The crystallographic data of complexes **2a**, **3a**, **3** and **6d** were collected on a Bruker AXSD8 diffractometer with a graphite-monochromatic Mo-Kα (λ = 0.71073 Å) radiation. All data were collected at 20 °C using omega-scan techniques. The structures of the complexes were solved by direct methods and refined using Fourier techniques. An absorption correction based on SADABS was applied for complex **2a** [61]. All non-hydrogen atoms were refined by full-matrix least-squares on *F*2 using the SHELXTL program package [62]. Hydrogen atoms were located and refined by the geometry method. The cell refinement, data collection, and reduction were done using Bruker SAINT [63]. The structure solution and refinement were performed with SHELXS-97 [64] and SHELXL-97 [65] respectively. Molecule structures were generated using ORTEP [66].

2.4. Ring-opening polymerization of cyclic esters

2.4.1. Typical polymerization procedure for rac-LA

To a solution of *rac*-lactide (288 mg, 2.00 mmol) in toluene (1.5 mL), the solution of aluminum complex (0.02 mmol) in toluene (0.5 mL) was added. The total volume was 2.0 mL. The mixture was then immerged into an oil bath at intended temperature and stirred for desired time interval. Polymerization aliquot was withdrawn under the protection of argon and quenched with methanol. After removal of the volatiles, the residue was subjected to ^{1}H NMR analysis. Monomer conversion was determined by observing the methine resonance integration of monomer vs. polymer in the ^{1}H NMR ($CDCl_3$, 400 MHz) spectrum. The bulk polymerization mixture was quenched at the same time with methanol. The purification of the polymer in each case was managed by dissolving the crude sample in CH_2Cl_2 and precipitating the polymer solution with methanol. The obtained polymers were further dried in a vacuum oven at 60 ºC for 24 h and subjected to GPC analysis and homonuclear decoupled ^{1}H NMR measurement.

2.4.2. Typical polymerization procedure for ε-CL

To a solution of *ε*-caprolactone (1.0 mL, 2.0 mmol) in toluene at 70 ºC, the solution of aluminum complex (0.02 mmol) in toluene (1.0 mL) was added. The mixture was then stirred for desired time interval at this temperature. Polymerization aliquot was withdrawn under the protection of argon and quenched with methanol. After removal of the volatiles, the residue was subjected to ^{1}H NMR analysis. Monomer conversion was determined by observing the integration of monomer *vs.* polymer methylene resonance in the ^{1}H NMR ($CDCl_3$, 400 MHz) spectrum. The bulk polymerization mixture was quenched at the same time by addition of methanol. The purification of the polymer in each case was managed by dissolving the crude samples in CH_2Cl_2 and precipitating the polymer solution with methanol. The obtained polymers were further dried in a vacuum oven at 60 ºC for 24 h and subjected to GPC analysis.

3. Results and discussion

3.1. Synthesis of ketiminate aluminum complexes

Various substituted ketimines $\mathbf{L^{1\text{-}6}H}$ could be easily prepared according to the published procedure by reacting a 1:1 ratio of 2, 4-pentandione and the corresponding substituted aniline in toluene under reflux conditions in the presence of *para*-toluenesulfonic acid as a catalyst [56,67-69]. Reactions of ketimines $\mathbf{L^{1\text{-}5}H}$ with trimethylaluminum in 1:1 molar ratio generated the target four-coordinated aluminum complexes (κ^2-OCMeCHCMeNAr)$AlMe_2$ (**1a-5a**) as illustrated in Scheme 1. The reactions proceeded smoothly along with the elimination of 1 equiv. of methane. The crude products were recrystallized by dissolving in minimum amount of toluene or a hexane-toluene mixture and kept at −20 °C for a few days. Analytically pure colorless powders or crystals of **1a**-**5a** could be obtained in moderate yields after filtration and repeated washing with hexane for several times. All the synthesized ketiminate aluminum dimethyl complexes **1a**-**5a** were characterized by ^{1}H and ^{13}C{^{1}H} NMR spectroscopy. While complexes **2a**, **4a** and **5a** were characterized by EA, complexes **1a** and **3a** were further characterized by HRMS since satisfied elemental analysis results could not be obtained even after several repeated recrystallization processes.

In the ^{1}H and ^{13}C NMR spectra of complexes **1a**-**5a**, the signals for proton and carbon of the methine group of the backbone serve as excellent indicators for evaluating the purity of these metal complexes. All the purified complexes show only one resonance attributable to the methine group of the backbone at ca. δ 5.2 ppm and ca. δ 98.0 ppm in the ^{1}H and ^{13}C NMR spectra, respectively. Besides, complexes **1a**-**5a** show a characteristic resonance for Al-CH_3

group at ca. δ –0.9 ppm and an integral ratio of Al-CH_3 and γ-C*H* being 6:1 in the ^{1}H NMR spectra, indicating the formation of mono(ketiminate) aluminum dimethyl complexes.

The reaction of ketimine **L^{6}H** bearing a *para*-CF_3 group on the *N*-phenyl ring with trimethylaluminum in 1:1 ratio was also attempted. The ^{1}H NMR spectrum of the resulting solid product indicated the presence of the target mono(ketiminate) aluminum dimethyl complex along with the bis(ketiminate) aluminum complex, which hindered the isolation of the pure target aluminum dimethyl complex. This might be due to the strong electron-withdrawing ability of CF_3 group causing significant electron deficiency on the phenyl ring and being in favor of the further reaction.

Similar reaction route was further applied to synthesize the corresponding bisligated aluminum complexes of proligands **L$^{1\text{-}6}$H** by allowing $AlMe_3$ to react with these ketimines in 1:2 ratio. It was found that harsh conditions of stirring at 90°C for 3 days had to be adopted. However, only ketimine **L^{2}H** bearing an *N*-2, 6-dichlorophenyl was converted to the target bisligated aluminum complex **2b** successfully (Scheme 2). In the ^{1}H NMR spectrum of complex **2b**, one singlet for the two γ-*CH* at δ 5.16 ppm and two double of doublets along with a triplet in the low field region are displayed, indicating a symmetric coordination mode of two ketiminate ligands. The existence of two dd signals accounting for protons in the *meta*-positions implies that for each phenyl ring the two *meta*-protons are chemically inequivalent, likely due to the restricted rotation of the phenyl ring. The characteristic resonance of Al-CH_3 protons for **2b** can be observed at δ –0.88 ppm, which is in 3:2 ratio with the γ-C*H* resonance.

From the reaction mixture of ketimine **L^{1}H** and $AlMe_3$ in 1:2 molar ratio, colorless crystals could be isolated which however proved to be a mixture of mono(ketiminate) complex **1a** and the target bis(ketiminate) complex **1b** as well as a small amount of proligand **L^{1}H** as characterized by

^{1}H NMR spectroscopy. Due to similar solubilities of three components, the isolation of analytically pure bisligated aluminum complex **1b** was failed.

The 1:2 ratio reaction of $AlMe_3$ with ketimine $\mathbf{L^3H}$ bearing an *N*-*p*-isopropylphenyl resulted in a reddish-brown solution after 3 days' reaction at 90 °C. After work-up, a white powder could be isolated from a petroleum ether solution. Unexpectedly, the ^{1}H NMR spectrum of this product shows no Al-CH_3 resonance, but displays more than expected signals (Fig. 1). The characteristic three types of γ-H resonances in 1:1:1 ratio together with three multiple resonances at 2.0~3.0 ppm accounting for the methine proton of the isopropyl group indicate clearly the presence of three types of ketiminate ligands. We therefore suggest that the stoichiometric structure of this product might be in the form of "Al(L^3)$_3$" (**3**, Scheme 3). To our surprise, in the same region of γ-H there is an additional doublet (4.5 ppm, J = 7.6 Hz) with an integral of one proton. Furthermore, only eleven aromatic protons instead of twelve protons are detected in the low field region. The doublet at 4.5 ppm has a similar coupling constant with these aromatic protons. All these features suggest that this doublet might be assignable to an aromatic proton as well. To further confirm the structure of complex **3**, single crystals suitable for *X*-ray diffraction study were obtained. The solid state structure of complex **3** (*vide post*) is in consistent with our assumption, where three ketiminate ligands surround the aluminum center in a *mer*-configuration [70] and an obvious shielding effect of one aromatic proton at the *ortho*-position by the adjacent phenyl ring is observed clearly. It is worthy of noting that, although the formation of aluminum complexes ligated with three *N*-thiophenol substituted ketiminate ligands was reported previously [71], a structural characterization of tri(ketiminate) aluminum complex and such unusual shielding effect have never been reported previously. Similar triligated aluminum complexes were also detected in the ^{1}H NMR spectra of the crude products of the reactions of

ketimines $\mathbf{L^{4\text{-}6}H}$ with $AlMe_3$. However due to the formation of a mixture of products, no analytically pure complex could be isolated. Possibly, ketimines with bulkier *N*-aryl substituent, for instance, 2,6-dichlorophenyl, favor the formation of bisligated aluminum complex, while ketimines with the less steric *p*-substituted *N*-aryl group create triligated complexes under harsh reaction conditions [72].

In order to obtain aluminum alkoxide complexes with ketiminate ligands, $Al(O^iPr)_3$ was used to react with these ketimine proligands at elevated temperature. From the reaction of proligand $\mathbf{L^2H}$ and $Al(O^iPr)_3$, the target bis(ketiminate) aluminum isopropoxide complex **2c** could be isolated as colorless crystalline solids in a moderate yield after recrystallization from a toluene solution at –20 °C. The ^{1}H NMR spectrum of **2c** shows a triplet and two doublets belonging to the aromatic protons in the range of δ 7.05~7.37 ppm. The resonance of two γ-H appears as a singlet at 5.26 ppm, indicating symmetric coordination geometry. The methine proton and methyl group of isopropoxide could be clearly identified. The integral ratio of isopropoxy group and γ-H of the ketiminate ligand is 1 : 2, giving evidence to the formation of bis(ketiminate) aluminum isopropoxide complex. Based on the literature reports regarding the molecular structures of many aluminum isopropoxide complexes [70], a dimeric structure bridged by two isopropoxyl groups is suggested for **2c** (Scheme 4).

The reaction of proligands $\mathbf{L^1H}$, $\mathbf{L^{3\text{-}6}H}$ with $Al(O^iPr)_3$ did not afford the target bis(ketiminate) aluminum isopropoxide complexes. The ^{1}H NMR spectra of isolated solids showed no presence of isopropoxide group in the structures. Instead, three singlets in 1:1:1 molar ratio account for three γ-*CH* protons appeared, indicating the formation of "AlL_3" complexes again. The solids obtained however were not clean enough, further recrystallization failed to provide analytical pure complexes. From the mother liquor of the reaction between $Al(O^iPr)_3$ and ketimine $\mathbf{L^6H}$, several

colorless single crystals were obtained, which were characterized by X-ray diffraction determination to be a binuclear aluminum isopropoxide complex **6d** (*vide post*), where the two aluminum centers are in different coordination environment. In order to obtain corresponding bis(ketiminate) aluminum isopropoxide complexes of proligands $\mathbf{L^1H}$, $\mathbf{L^{3\text{-}6}H}$, different reaction conditions were adopted, but all proved to be unsuccessful. By monitoring the NMR scale reaction of $\mathbf{L^6H}$ and $Al(O^iPr)_3$ in a 2:1 molar ratio, the formation of triligated complex **6** as the major product companied by a small amount of **6d** was detected upon gentle warming the reaction mixture, but no reaction took place at ambient temperature, indicating that the target aluminum isopropoxide complex "$(L^6)_2Al(O^iPr)$" is either thermodynamically unstable or more reactive than the staring precursor which leads to the formation of the more stable triligated complex **6** as the major product.

3.2. Crystal structures of aluminum complexes

Single crystals of complexes **2a**, **3a** and **3** were obtained from a saturated toluene solution or a hexane-toluene mixture, or a saturated petroleum ether solution at −20 °C, respectively. The unanticipated complex **6d** was isolated from the reaction mixture of $Al(O^iPr)_3$ and $\mathbf{L^6H}$, and suitable single crystals were successfully obtained from a toluene solution at −20°C. A summary of crystal and refinement data for **2a**, **3a**, **3** and **6d** are listed in Table 1.

Crystallographic data indicates that **2a** possesses a tetra-coordinate metal core surrounded by the oxygen and nitrogen atoms of the chelating ketiminate ligand and two methyl groups in a distorted tetrahedral environment (Fig. 2). The biting angle of the ketiminate ligand, N(1)–Al(1)–O(1) = 95.19(8)°, is significantly smaller than the regular tetrahedral bond angle of 109.5°. However, it is still in the normal range of 86.76~100.04° for the tetra-coordinate β-diketiminate metal complexes. The bond lengths between atoms of the ketiminate backbone are all in the

same ranges, which are comparable to those of aluminum ketiminate complexes reported by Huang's group [14]. The C(2)–Al(1)–C(1) bond angle of 117.79(16)° and lengths of Al1–O1 (1.7836(18) Å), and Al1–N1 (1.9438(18) Å) are slightly smaller than the corresponding bond angle and lengths of mono(ketiminate) aluminum complex bearing *N*-2,6-isopropylphenyl substitution reported by Huang [15]. The significant shortness of Al1–O1 bond length in comparison with Al1-N1 bond length indicates higher covalent nature of this bond.

In the solid state, the crystal of complex **3a** belongs to the orthorhombic crystal system. The aluminum center, being surrounded by the nitrogen and oxygen donors of the chelating ketiminate ligand and two methyl groups, possesses a distorted tetrahedral geometry as observed in **2a** (Fig. 3). All the structure parameters are quite similar to those of **2a**, except that the length difference between Al1–O1 and Al1–N1 bonding is slightly smaller than that of **2a**, indicative of a more averaged donation effect likely attributable to the *N*-aryl with an electron donating isopropyl group. The bond length of N1–C8 in **3a** is 1.446(3) Å, which is also slightly longer than the one in **2a** (N1–C8 =1.427(2) Å).

The molecular structure of **3** features a six coordinate aluminum center in a slightly distorted octahedral geometry with the bond angles O(2)–Al(1)–O(3) = 178.80(5)°, N(1)–Al(1)–N(2) = 177.25(5)° and O(1)–Al(1)–N(3) = 174.32° deviating slightly from 180° (Fig. 4). Expectedly, the higher electronegativity of oxygen atom results in more covalent nature of the Al–O bonds than that of Al–N bonds, and thus shorter bond lengths are observed for Al–O bonds (Al1–O1 1.8764(10) Å, Al1–O2 1.8321(9) Å, Al1–O3 1.8488(9) Å; Al1–N1 2.0403(11) Å, Al1–N2 2.0524(11) Å, Al1–N3 2.0671(11) Å). However, Al1–O bond lengths and the angles are still comparable with previously reported octahedral $Al(acac)_3$ (Al–O = 1.892 Å) [69] and $Al(hfacac)_3$

(Al–O = 1.873-1.883 Å) complexes [73]. As shown in Fig. 4, three ketiminate ligands in complex **3** surround the aluminum center in a *mer*-configuration, which is supposed to reduce the steric repulsion among the ligands more effectively than the likely *fac*-isomer.

As shown in Fig. 5, the crystal structure of the dinuclear aluminum complex **6d** exhibits six- and four-coordinated aluminum centers bridged by two μ-isopropoxide groups. The whole molecular has C_2-symmetry with an axis defined by the two aluminum centers. The aluminum center bearing two ketiminate ligands lies in a distorted octahedral environment with the bond angles significantly deviated from the ideal values of 90° and 180° for octahedral geometry (O1–Al1–O1* 98.90(13)°, O1–Al1–O2* 167.81(9)°, N1–Al1–N1* 168.48(13)°). Consistently, Al–O (ketiminate) bonds are more covalent than Al–N bonds because of the more electronegative nature of oxygen atom (Al1–O1/Al1-O1* 1.8255(19) Å; Al1–N1/Al1-N1* 2.080(2) Å). The other aluminum center bearing two isopropoxide groups lies in a tetrahedral environment with the bond angles also deviated from the regular bond angle of 109.5° (O3–Al2–O3* 116.67(18)°, O3–Al2–O2 118.38(11)°, O2–Al2–O2* 81.14(12)°). The distances between the octahedral aluminum center and the oxygen atoms of the bridged isopropoxide groups (Al1–O2/Al1–O2*, 1.9231(19) Å) are significantly longer than those between the tetrahedral aluminum center and the μ-oxygen atoms (Al2–O2/Al2-O2*, 1.791(2) Å) owing to the less electrophilic nature of the former aluminum center. The spatial distance between two metal centers in **6d** (Al1⋯⋯Al2 = 2.89 Å) is similar to that in the previously reported aluminum complex [(hfacac)Al(μ-$O^iPr)_2$Al(hfacac)] (Al(1)⋯⋯Al(2) = 2.86 Å) where two aluminum centers with the same coordination geometry are involved [70].

3.3. Ring-opening polymerization of rac-LA

Aluminum methyl complexes **1a**-**5a** and **2b** were employed in the ROP of *rac*-LA as single component initiator and were proved to be active catalysts for the ROP of *rac*-LA at 70 °C, but inactive below that temperature. The position and nature of substituents on the *N*-phenyl ring have considerable influence on the catalytic activity and selectivity of the corresponding aluminum complexes.

As shown in Table 2, the polymerization of *rac*-LA initiated by aluminum dimethyl complex **1a** with *N*-(2,6-dimethlyphenyl)ketiminate ligand reached 56% of monomer conversion in 72 h, which was found to be the least active catalyst in this group (run 2). On the contrary, complex **2a** could achieve almost full monomer conversion within 72 h. The introduction of electronegative Cl atoms at 2,6-positions of phenyl ring instead of methyl groups resulted in a significant increase in the catalytic activity. In other words, methyl as an electron-donating group on 2,6-positions of the phenyl ring decreased the electrophilicity of the aluminum center through the chelating π-system of ancillary ligand, and thus became a disadvantage for the coordination of monomer, leading to a decrease in the activity. Activities of complexes **3a** (*p*-^{i}Pr), **4a** (*p*-OMe) and **5a** (*p*-Cl) were investigated in the same group and an increasing tendency of catalytic activities was found as **3a** (*p*-OMe) < **4a** (*p*-^{i}Pr) < **5a** (*p*-Cl). Complex **5a** was also the most active catalyst among **1a**-**5a** by reaching 97% of monomer conversion in 48 h (Run 10). The data is consistent with the polymerization results reported by Huang [14], the bisligated aluminum complex **2b** was proved to be more active than the corresponding mono(ketiminate) complex **2a**, by converting 90% of monomer in 24 h.

The polymerization of *rac*-LA initiated by aluminum complexes **1a-5a** and **2b** afforded high molecular weight polymers with broad polydispersities. In most of the cases, the measured number average molecular weights deviate significantly from the theoretical values. As indicated

in Table 2, all the complexes resulted in isotactic-enriched PLAs at 70 °C. PLAs produced by **1a** and **2a** (P_m = 0.70-0.72) display higher isotacticities than those obtained by aluminum complexes **3a**-**5a** bearing ketiminates of *N*-*para*-substituted phenyl (P_m = 0.57~0.60). In other words, the introduction of a substituent on the *para*-position instead of *ortho*-positions decreases the isotactic selectivity. This can be explained by the steric effect of substituents on *ortho*-positions, causing bulkiness and blocking partially the coordination sphere of the metal center to direct the monomer insertion. Besides, the bis(ketiminate) aluminum complex **2b** resulted in polylactides with similar isotacticity as the mono(ketiminate) aluminum complex **2a** of the same ligand.

A significant increase of catalytic activities was observed for these complexes with the addition of isopropanol into the system (See ESI, Table S1). The polymers obtained showed hydroxyl and isopropoxide signals in 1:6 ratio in their ^{1}H NMR spectra, indicating the formation of linear PLAs end-chapped with hydroxyl and isopropoxide terminals. The crucial effect of ^{i}PrOH on the polymerization prompted us to monitor the reaction via ^{1}H NMR spectroscopy. After addition of lactide monomer and isopropanol to **2a** in $CDCl_3$ at r.t. ([*rac*-LA]:[^{i}PrOH]:[**2a**] = 10:1:1), signals attributable to the free ligand $\mathbf{L^2H}$ appeared in the ^{1}H NMR spectrum along with Al-OC*H*(CH_3)$_2$ proton signals and a new Al-C*H*$_3$ signal at −0.78 ppm. Besides, small amount of **2a** and some other species in low content also existed. The signals of lactide monomer were unchanged until the mixture was heated at 50 °C for 24 h to display the characteristic resonances of PLA. It was clear that the added isopropanol reacted with the aluminum complex to kick out the free ligand as a dominant pathway and meanwhile new aluminum species such as "AlMe$_2$(O^{i}Pr)" and "AlMe(O^{i}Pr)$_2$" were formed, which initiated the ROP of *rac*-lactide instead. Similar result was reported previously for amidinate aluminum

complexes [74]. The presence of multiple active species also gave the explanation on the broad molecular weight distributions obtained even with the addition of alcohol.

Aluminum alkoxide complexes can be classified into a group which includes the most useful catalysts for lactide polymerization [10-12,27]. Supporting the previous studies, as a single component aluminum alkoxide initiator, aluminum isopropoxide complex **2c** exhibited significantly higher catalytic activity than aluminum methyl complexes **1a**-**5a** and **2b** for the ROP of *rac*-LA at 70 °C in toluene, and high monomer conversions were observed within 12 h, indicating that the metal-alkoxide bond is very active for ROP by exerting sufficient nucleophilic attack on the monomer in initiation. From the data listed in Table 2, it is found that the polymerization still afforded PLA with relatively broad molecular weight distribution (M_w/M_n = 1.6), but the molecular weight of the polymer sample is comparable to the calculated one. Being different from the bis(ketiminate) aluminum methyl complex **2b**, complex **2c** is less stereoselective for the ROP of *rac*-LA and provides PLA with dominantly atactic microstructure (P_m = 0.56). Obviously different active species should be involved in the polymerization, and the dimeric structure of complex **2c** is likely to be responsible for the decrease of the isotactic selectivity. Furthermore, the polymer obtained from the polymerization of *rac*-LA initiated by complex **2c** shows clearly hydroxyl and isopropoxide signals in 1:6 ratio in the ^{1}H NMR spectrum, indicating the formation of linear PLA end-chapped with hydroxyl and isopropoxide terminals.

3.4. Ring-opening polymerization of ε-CL

Complexes **1a-5a**, **2b** and **2c** are also active for the ROP of ε-CL. As shown in Table 3, in general the polymerizations of ε-CL initiated by these ketiminate aluminum complexes were faster than those of *rac*-LA, and could be completed within 12 hours at 70 °C. Unlike the polymerization of *rac*-LA, the electronic effect of substituents at the *N*-phenyl ring of the ligand

framework on the catalytic activity of the corresponding aluminum complex is not conclusive. Complexes **1a** (*o*-Me_2) and **2a** (*o*-Cl_2) with an *ortho*-substituted *N*-phenyl group exhibited almost the same activity. However, the bis(ketiminate) aluminum methyl complex **2b** was found to be significantly more active than all the other aluminum complexes by completing the polymerization in 5 h under otherwise identical conditions. By using complex **2a** (*o*-Me_2) as initiator, ε-CL conversion up to 65% could be obtained in 3 days at 25 °C, while 98% of monomer conversion was obtained in 1 day at 50 °C.

It is found that the measured molecular weights of resultant polymers obtained by complexes **1a**-**5a** and **2b** significantly deviate from the theoretical values and the molecular weight distributions are rather broad (PDI = 1.8~2.4). In contrast, aluminum isopropoxide complex **2c** affords polymers with relatively narrow molecular weight distribution (PDI = 1.3) and the molecular weight is much more comparable to the theoretical value. All these suggest that ROPs of ε-CL initiated by these aluminum methyl complexes are not well controlled in comparison to those initiated by aluminum isopropoxide complex.

4. Conclusions

Aluminum methyl complexes **1a**-**5a** and **2b** bearing ketiminate ligands were synthesized from the reactions of trimethylaluminum and the corresponding ketimines. Two of them were further identified by X-ray crystallography. Bis(ketiminate) aluminum isopropoxide complex **2c** was also obtained from the reaction of the corresponding ketimine with $Al(O^iPr)_3$ under harsh conditions. The reactions of $AlMe_3$ or $Al(O^iPr)_3$ with ketimines bearing *para*-substituted *N*-phenyl group often led to the formation of triligated aluminum complexes as the major products, with typical complex **3** characterized by a X-ray diffraction study. All the aluminum methyl

515 complexes were proved to be active catalysts in the ring-opening polymerization of *rac*-LA and ε-
516 CL at high temperature to yield high molecular weight polymers with broad polydispersities.
517 While the substitution on the ketiminate ligand affected the reactivity and stereoselectivity of these
518 complexes for *rac*-LA polymerization, it did not show a conclusive effect on the polymerization
519 of ε-CL monomer. Aluminum isopropoxide complex **2c** exerted better control for the ROP of
520 *rac*-LA and ε-CL, producing polymers with relatively narrow molecular weight distribution and
521 smaller molecular weights which are comparable to the theoretical values.

522

523 **Appendix A. Supplementary data**

524 CCDC 984641-984644 contain the supplementary crystallographic data for **2a**, **3a**, **3** and **6d**,
525 respectively. These data can be obtained free of charge via
526 www.ccdc.cam.ac.uk/conts/retrieving.html, or from the Cambridge Crystallographic data Centre,
527 12 Union Road, Cambridge CB2 1EZ, UK; fax: +44 1223 336 033; or email:
528 deposit@ccdc.cam.ac.uk.

529

530 **Acknowledgments**

531 This work is subsidized by the National Natural Science Foundation of China (NNSFC,
532 20604009 and 21074032), and the Fundamental Research Funds for the Central Universities
533 (WK1214048, WD1113011). All the financial supports are gratefully acknowledged. H. Ma
534 also thanks the very kind donation of a Braun glove-box by AvH foundation.

535

536 **References**

537 [1] T. Hayashi, Prog. Polym. Sci. 19 (1994) 663.

538 [2] R. G. Sinclair, Pure Appl. Chem. A33 (1996) 585.

[3] E. Chiellini, R. Solaro, Adv. Mater. 8 (1996) 305.

[4] W. Amass, A. Amass, B. Tighe, Polym. Int. 47 (1998) 89.

[5] Y. Ikada, H. Tsuji, Macromol. Rapid Commun. 21 (2000) 117.

[6] J. C. Middlenton, A. J. Tipton, Biomaterials 21 (2000) 2335.

[7] R. Langer, Acc. Chem. Res. 33 (2000) 94.

[8] M. Vert, G. Schwarch, G. Coudane, J. Pure Appl. Chem. A32 (1995) 787.

[9] K. Sudesh, T. Iwata, Clean 36 (2008) 433.

[10] O. D.-Cabaret, B. M.-Vaca, D. Bourissou, Chem. Rev. 104 (2004) 6147.

[11] M. J. Stanford, A. P. Dove, Chem. Soc. Rev. 39(2010) 486.

[12] C. M. Thomas, Chem. Soc. Rev. 39 (2010) 165.

[13] D. Chakraborty, E. Y.-X. Chen, Organometallics 21 (2002) 1438.

[14] R.-C. Yu, C.-H. Hung, J.-H. Huang, H.-Y. Lee, J.-T. Chen, Inorg. Chem. 41 (2002) 6450.

[15] T.-L. Yu, T.-L. Huang, L.-F. Yang, B.-T. Ko, C.-C. Lin, J. Chin. Chem. Soc. 47 (2000) 1185.

[16] C.-H. Huang, F.-C. Wang, B.-T. Ko, T.-L. Yu, C.-C. Lin, Macromolecules 34 (2001) 356.

[17] B. Lian, C. M. Thomas, O. L. Casagrande Jr., C. W. Lehmann, T. Roisnel, and J.-F. Carpentier, Inorg. Chem. 46 (2007) 328.

[18] E. L. Whitelaw, G. Loraine, M. F. Mahon, M. D. Jones, Dalton Trans. 40 (2011) 11469.

[19] W. Li, W. Wu, Y. Wang, Y. Yao, Y. Zhang, Q. Shen, Dalton Trans. 40 (2011) 11378.

[20] S. Qiao, W.-A. Ma, Z.-X. Wang, J. Organomet. Chem. 696 (2011) 2746.

[21] K. Matsubara, C. Terata, H. Sekine, K. Yamatani, T. Harada, K. Eda, M. Dan, Y. Koga, M. Yasuniwa, J. Polym. Sci., Part A, Polym. Chem. 50 (2012) 957.

561 [22] C. Bakewell, R. H. Platel, S. K. Cary, S. M. Hubbard, J. M. Roaf, A. C. Levine, A. J. P.
562 White, N. J. Long, M. Haaf, C. K. Williams, Organometallics 31 (2012) 4729.
563 [23] M. Normand, V. Dorcet, E. Kirillov, J.-F. Carpentier, Organometallics 32 (2013) 1694.
564 [24] C. P. Radano, G. L. Baker, M. R. Smith, III, J. Am. Chem. Soc. 122 (2000) 1552.
565 [25] T. M. Ovitt, G. W. Coates, J. Polym. Sci. A: Polym. Chem. 38 (2000) 4686.
566 [26] B.-T. Ko, C.-C. Lin, Macromolecules 32 (1999) 8296.
567 [27] Y.-C. Liu, B.-T. Ko, C.-C. Lin, Macromolecules, 34 (2001) 6196.
568 [28] M.-L. Hsueh, B.-H. Huang, C.-C. Lin, Macromolecules 35 (2002) 5763.
569 [29] C.-T. Chen, C.-A. Huang, B.-H. Huang, Macromolecules 37 (2004) 7968.
570 [30] K. Phomphrai, P. Chumsaeng, P. Sangtrirutnugul, P. Kongsaeree, M. Pohmakotr, Dalton
571 Trans. 39 (2010) 1865.
572 [31] K. Phomphrai, P. Chumsaeng, P. Sangtrirutnugul, P. Kongsaeree, M. Pohmakotr, Dalton
573 Trans. 39 (2010) 1865–1871.
574 [32] A. D. Schwarz, Z. Chu, P. Mountford, Organometallics 29 (2010) 1246.
575 [33] J. S. Klitzke, T. Roisnel, E. Kirillov, O. de L. Casagrande, Jr., and J.-F. Carpentier,
576 Organometallics 33 (2014) 309.
577 [34] A. Le Borgne, V. Vincens, M. Jouglard, N. Spassky, Macromol. Chem., Macromol. Symp.
578 73 (1993) 37.
579 [35] G. Montaudo, M. S. Montaudo, C. Puglisi, F. Samperi, N. Spassky, A. Le Borgne,
580 Macromolecules 29 (1996) 6461.
581 [36] N. Spassky, M. Wisniewski, C. Pluta, A. LeBorgne, Macromol. Chem. Phys. 197 (1996)
582 2627.
583 [37] T. M. Ovitt, G. W. Coates, J. Am. Chem. Soc. 121 (1999) 4072.

584 [38] T. M. Ovitt, G. W. Coates, J. Am. Chem. Soc. 124 (2002) 1316.

585 [39] Z. Zhong, P. J. Dijkstra, J. Feijen, Angew. Chem. Int. Ed. 41 (2002) 4510.

586 [40] Z. Zhong, P. J. Dijkstra, J. Feijen, J. Am. Chem. Soc. 125 (2003) 11291.

587 [41] N. Nomura, R. Ishii, M. Akahura, K. Aoi, J. Am. Chem. Soc. 124 (2002) 5938.

588 [42] N. Nomura, R. Ishii, Y. Yamamoto, T. Kondo, Chem. Eur. J. 13 (2007) 4433.

589 [43] W. Li, Y. Yao, Y. Zhang, Q. Shen, Chin. J. Chem., 30 (2012) 609.

590 [44] Z. Tang, X. Chen, X. Pang, Y. Yang, X. Zhang, X. Jing, Biomacromolecules 5 (2004) 965.

591 [45] H. Du, X. Pang, H. Yu, X. Zhuang, X. Chen, D. Cui, X. Wang, X. Jing, Macromolecules,
592 40 (2007) 1904.

593 [46] M. H. Chisholm, N. J. Patmore, Z. Zhou, Chem. Commun. (2005) 127.

594 [47] M. H. Chisholm, J.C. Gallucci, K. T. Quisenberry, Z. Zhou, Inorg. Chem. 47 (2008) 2613.

595 [48] H.-L. Chen, S. Dutta, P.-Y. Huang, C.-C. Lin, Organometallics 31 (2012) 2016.

596 [49] P. Hormniru, E. L. Marshall, V. C. Gibson, A. J. P. White, D. J. Williams, J. Am. Chem.
597 Soc. 126 (2004) 2688.

598 [50] H. Du, A. H. Velders, P. J. Dijkstra,; J. Sun, Z. Zhong, X. Chen, J. Feijen, Chem. Eur. J. 15
599 (2009) 9836.

600 [51] X. Pang, H. Du, X. Chen, X. Zhuang, D. Cui, X. Jing, J. Polym. Sci. A Polym. Chem. 43
601 (2005) 6605.

602 [52] X. Pang, H. Du, X. Chen, X. Wang, X. Jing, Chem. Eur. J. 14 (2008) 3126.

603 [53] A. Alaaeddine, C. M. Thomas, T. Roisnel, J.-F. Carpentier, Organometallics 28 (2009) 1469.

604 [54] D. J. Darensbourg, O. Karroonnirun, Organometallics 29 (2010) 5627.

605 [55] K. Fukushima, Y. Kimura, Polym. Int. 55 (2006) 626.

606 [56] S. Gong, H. Ma, Dalton Trans. (2008) 3345.

[57] K. Bakthachalam, N. D. Reddy, Organometallics 32 (2013) 3174.

[58] D. Kong, Y. Peng, D. Li, P. Chen, J. Qu, Inorg. Chem. Commun. 22 (2012) 158.

[59] J. Vela, L. Zhu, C. J. Flaschenriem, W. W. Brennessel, R. J. Lachicotte, P. L. Holland, Organometallics 26 (2007) 3416.

[60] D. Li, Y. Peng, C. Geng, K. Liu, D. Kong, Dalton Trans. 42 (2013) 11295.

[61] SADABS, Bruker Nonius area detector scaling and absorption correction-V2.05, Bruker AXS Inc., Madison, WI, 1996.

[62] G. M. Sheldrick, SHELXTL 5.10 for windows NT, Structure Determination Software Programs, Bruker Analytical X-ray Systems, Inc., Madison, WI, 1997.

[63] SAINT, Version 6.02, Bruker AXS Inc., Madison, WI, 1999.

[64] G. M. Sheldrick, SHELXS-97, Program for the Solution of Crystal Structures, University of Gottingen, Germany, 1990.

[65] G. M. Sheldrick, SHELXL-97, Program for the Refinement of Crystal Structures, University of Gottingen, Germany, 1997.

[66] C. K. Johnson, ORTEP-II: A FORTRAN Thermal Ellipsoid Plot Program for Crystal Structure Illustrations, Report ORNL- 5138, Oak Ridge National Laboratory, Oak Ridge, TN, USA, 1976.

[67] J. E. Parks, R. H. Holm, Inorg. Chem. 7 (1968) 1408.

[68] P. B. Hitchcock, M. F. Lappert, M. Layh, Chem. Commun. 2 (1998) 201.

[69] W. Clegg, E. K. Cope, A. J. Edwards, F. S. Mair, Inorg. Chem. 37 (1998) 2317.

[70] M. Bouyahyi, T. Roisnel, J.-F. Carpentier, Organometallics 29 (2010) 491.

[71] S. Sharma, R. Sharma, R. Sharma, A. Sharma, A. K. Rai, Bioinorgan. Chem. Appl. 1 (2003) 215.

630 [72] K. H. Park, W. J. Marshall, J. Org. Chem. 70 (2005) 2075.

631 [73] P. K. Hon, C. E. Pfluger, J. Coord. Chem. 3 (1973) 67.

632 [74] F. Qian, K. Liu, H. Ma, Dalton Trans. 39 (2010) 8071.

633

634 Table 1

635 Crystal data and structure refinement details for complexes **2a**, **3a**, **3** and **6d**.
636

	2a	**3a**	**3**	**6d**
Empirical formula	$C_{13}H_{16}AlCl_2NO$	$C_{16}H_{24}AlNO$	$C_{42}H_{54}AlN_3O_3$	$C_{36}H_{50}Al_2F_6N_2O_6$
Formula weight	300.15	273.34	675.86	774.74
Temperature (K)	293(2)	296(2)	140(2) K	293(2) K
Wavelength (Å)	0.71073	0.71073	0.71073 Å	0.71073
Crystal system	Monoclinic	Orthorhombic	Triclinic	Monoclinic
Space group	P2(1)/n	Pbca	P -1	C 2/c
Crystal size (mm)	$0.25 \times 0.15 \times 0.15$	$0.30 \times 0.25 \times 0.20$	$0.20 \times 0.15 \times 0.10$	$0.32 \times 0.17 \times 0.14$
a (Å)	8.449(4)	9.6152(9)	9.5653(8)	11.210(2)
b (Å)	12.819(6)	16.9484(17)	14.1687(12)	20.209(4)
c (Å)	14.223(6)	21.394(2)	14.7347(12)	18.501(3)
α (°)	90	90	103.0320(10)	90
β(°)	91.235(5)°	90	92.335(2)	102.105
γ(°)	90	90	90.301	90
V (A^3)	1540.2(12)	3486.3(6)	1943.7(3)	4098.1(13)
Z	4	8	2	4
ρ (mg/m^3)	1.294	1.042	1.155	1.256
μ (mm^{-1})	0.467	0.110	0.093	0.141
F (000)	624	1184	728	1632
θ range (°)	2.14 to 27.00	2.40 to 25.05	1.420 to 30.565°	4.408 to 44.553°
Data collected (*hkl*)	±10, –16 to 13, –15 to18	±11, –19 to 20, –23 to 25	–11 to 13, ±20, –20 to 21	±13, –21 to 24, –22 to 20
Reflns collected/unique	7146/3262	16909/3089	19399/11746	12323/2901
R (int)	0.0424	0.0248	0.0190	0.0812
Data/restraints/params	3262/0/168	3089/0/178	11746/24/454	4026/184/307
Goodness-of-fit on F^2	1.013	1.027	1.057	1.037
Final R_1, wR_2 [I > 2σ(I)]	0.0504, 0.1383	0.0570, 0.1610	0.0507, 0.1541	0.0584, 0.1560
R_1, wR_2 (all data)	0.0679, 0.1504	0.0814, 0.1859	0.0644, 0.1747	0.0812, 0.1714
$\Delta\rho_{max,\ min}$/e $Å^{-3}$	0.319, –0.382	0.391, –0.268	0.934, –0.629	

637
638
639

Table 2

ROP of *rac*-LA initiated by ketiminate aluminum complexes [a]

Entry	Catalyst	Time (h)	Conv. (%)	$M_{n,calcd}$ [b] ($\times 10^4$)	M_n [c] ($\times 10^4$)	M_w/M_n [c]	P_m [d]
1	**1a** (*o*-Me_2)	24	21	0.30			
2		72	56	0.81	4.54	2.1	0.72
3	**2a** (*o*-Cl_2)	24	61	0.88			
4		72	97	1.40	3.43	2.1	0.70
5	**3a** (*p*-^{i}Pr)	24	36	0.52			
6		72	77	1.11	8.06	2.4	0.58
7	**4a** (*p*-OMe)	24	39	0.56			
8		72	86	1.24	4.68	1.9	0.60
9	**5a** (*p*-Cl)	24	85	1.23			
10		48	97	1.40	3.36	1.6	0.57
11	**2b** (*o*-Cl_2)	12	48	0.69			
12		24	90	1.30	6.93	1.9	0.70
13	**2c** (*o*-Cl_2)	8	86	1.24			
14		12	95	1.37	1.60	1.6	0.56

[a] $[rac\text{-LA}]_0/[Al]_0 = 100$, $[rac\text{-LA}]_0 = 1.0$ M, toluene, 70 °C.

[b] $M_{n,calcd} = ([rac\text{-LA}]_0/[Al]_0) \times 144.13 \times$ conv.%.

[c] Determined by gel permeation chromatography (GPC) in THF, calibrated with polystyrene standards.

[d] P_m is the probability of forming a new *m*-dyad, determined by homonuclear decoupled ^{1}H NMR spectroscopy.

Table 3

ROP of ε-CL initiated by ketiminate aluminum methyl complexes [a]

Entry	Catalyst	Time (h)	Conv. [b] (%)	$M_{n,calcd}$ [c] ($\times 10^4$)	M_n [d] ($\times 10^4$)	M_w/M_n [d]
1	**1a** (*o*-Me_2)	4	18	0.21		
2		12	97	1.11	6.24	2.1
3	**2a** (*o*-Cl_2)	4	18	0.21		
4		12	98	1.12	4.91	2.2
5[e]		12	50	0.57		
6[e]		24	98	1.12		
7[f]		72	65	0.74		
8	**3a** (*p*-^{i}Pr)	4	38	0.43		
9		12	96	1.09	4.88	1.8
10	**4a** (*p*-OMe)	4	24	0.27		
11		12	91	1.04	4.45	2.4
12	**5a** (*p*-Cl)	4	32	0.37		
13		12	94	1.07	9.84	1.8
14	**2b** (*o*-Cl_2)	4	70	0.79	9.27	1.8
15		5	99	1.14		
16	**2c**(*o*-Cl_2)	4	49	0.56		
17		8	99.6	1.14	0.90	1.3

[a] $[\varepsilon\text{-CL}]_0/[Al]_0 = 100$, $[\varepsilon\text{-CL}]_0 = 1.0$ M, toluene, $T = 70$ °C.
[b] Determined by ^{1}H NMR spectroscopy.
[c] $M_{n,calcd} = [\varepsilon\text{-CL}]_0/[Al]_0 \times 114 \times$ conv.%.
[d] Determined by gel permeation chromatography in THF, calibrated with polystyrene standards.
[e] $T = 50$ °C.
[f] $T = 25$ °C.

664 Scheme 1. Synthesis of mono(ketiminate) aluminum dimethyl complexes.
665
666

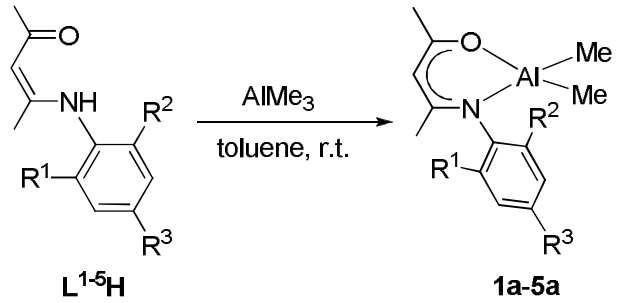

$L^{1\text{-}5}H$ **1a-5a**

L^1H, **1a**: $R^1 = R^2 = CH_3$, $R^3 = H$
L^2H, **2a**: $R^1 = R^2 = Cl$, $R^3 = H$
L^3H, **3a**: $R^1 = R^2 = H$, $R^3 = CH(CH_3)_2$
L^4H, **4a**: $R^1 = R^2 = H$, $R^3 = OCH_3$
L^5H, **5a**: $R^1 = R^2 = H$, $R^3 = Cl$

667
668

669 Scheme 2. Synthesis of bis(ketiminate) aluminum methyl complex **2b**.
670
671

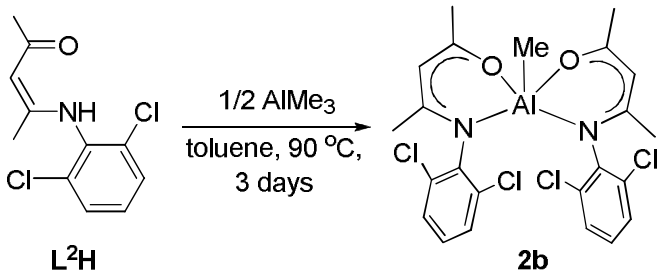

L^2H **2b**

672
673
674
675
676

677 Scheme 3. Synthesis of tri(ketiminate) aluminum complex **3**.
678
679

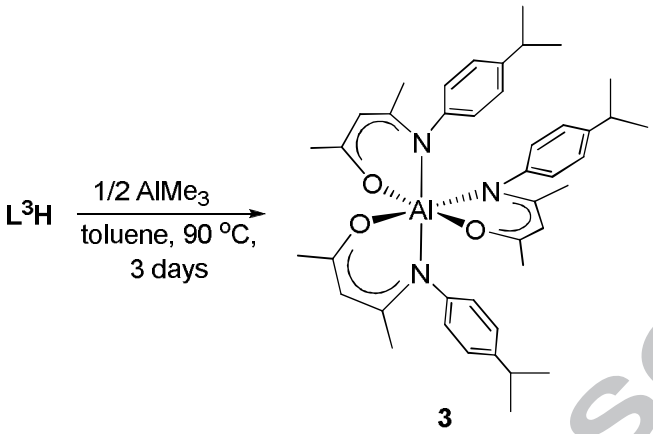

3

680
681
682

683 Scheme 4. Synthesis of bis(ketiminate) aluminum isopropoxide complex **2c**.
684
685

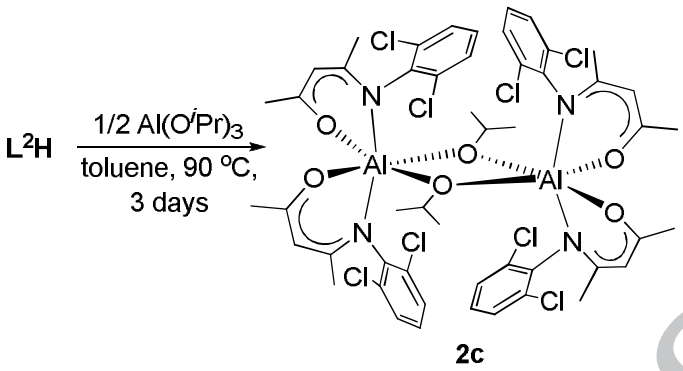

686
687

688 Scheme 5. The reaction of **L^{6}H** and Al(O^{i}Pr)$_3$ gave a mixture of **6** and **6d**.

689

690

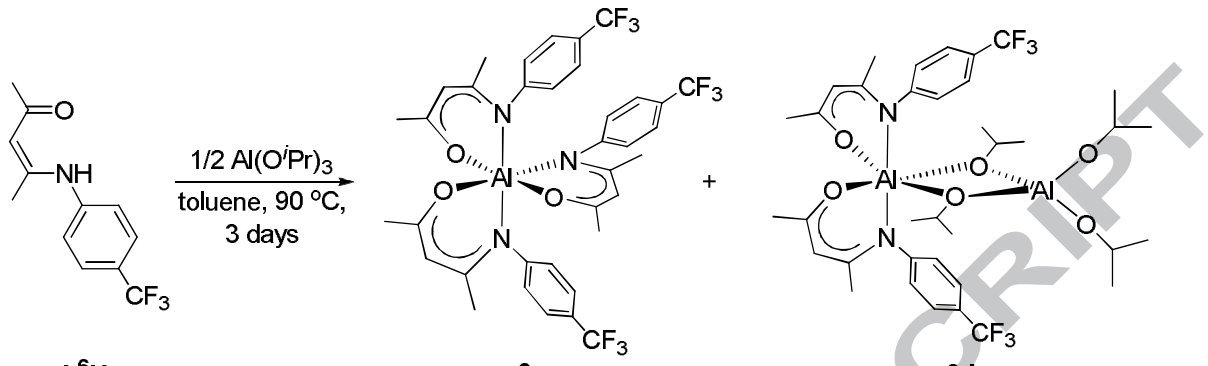

L^{6}H **6** **6d**

691

692

693 Fig. 1. ^{1}H NMR spectrum of complex **3** ($CDCl_3$, 400 MHz, 25 °C).

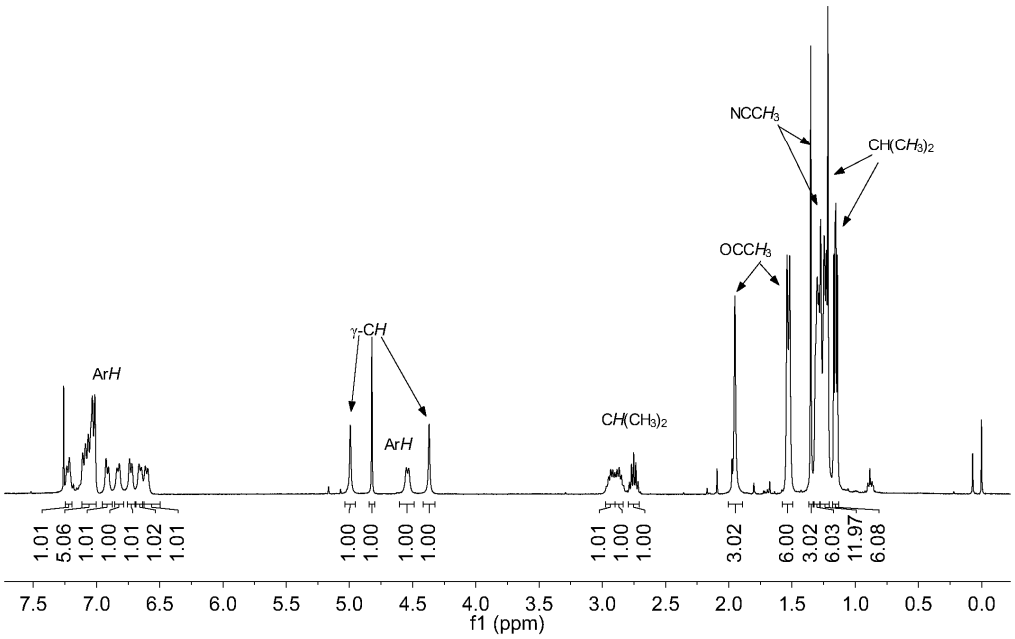

694
695

Fig. 2. Molecular structure of complex **2a**. Thermal ellipsoids are drawn at the 30% probability level. Hydrogen atoms on carbon atoms are omitted for clarity. Selected bond lengths [Å] and bond angles [°]: Al1–O1 1.7836(18), Al1–N1 1.9438(18), Al1–C1 1.945(3), Al1–C2 1.952(3), N1–C6 1.315(3), N1–C8 1.427(2), O1–C4 1.286(3), O1–Al1–N1 95.19(8), O1–Al1–C1 110.20(13), N1–Al1–C1 111.43(12), O1–Al1–C2 108.87(14), N1–Al1–C2 111.01(11), C1–Al1–C2 117.79(16), C6–N1–C8 119.35(17), C6–N1–Al1 123.37(15), C8–N1–Al1 117.27(13), C4–O1–Al1 128.40(16).

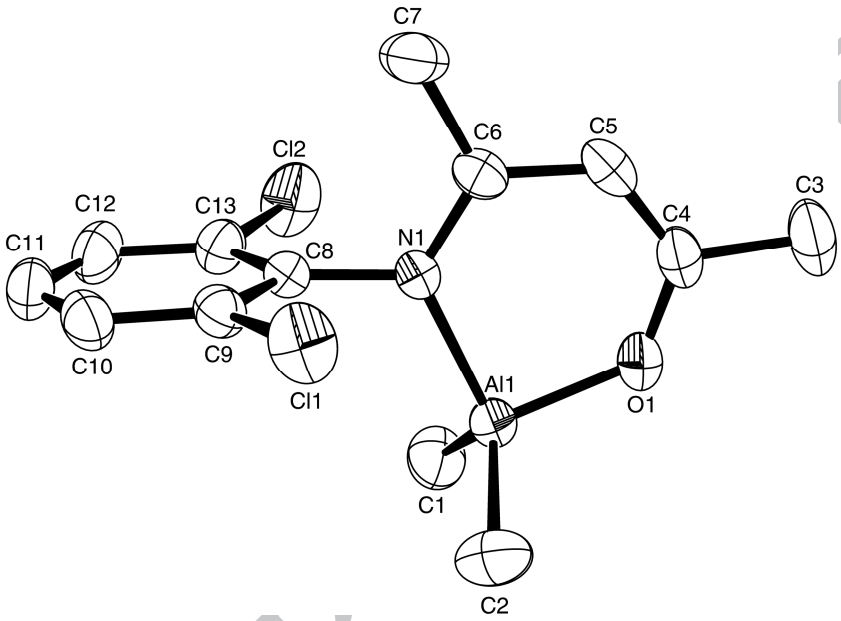

Fig. 3. Molecular structure of complex **3a**. Thermal ellipsoids are drawn at the 30% probability level. Hydrogen atoms on carbon atoms are omitted for clarity. Selected bond lengths [Å] and bond angles [°]: Al1–O1 1.792(2), Al1–N1 1.937(2), Al1–C1 1.946(3), Al1–C2 1.961(4), O1–Al1–N1 95.33(10), O1–Al1–C1 111.72(15), N1–Al1–C1 110.31(14), O1–Al1–C2 110.44(16), N1–Al1–C2 109.99(14), C1–Al1–C2 116.95(18).

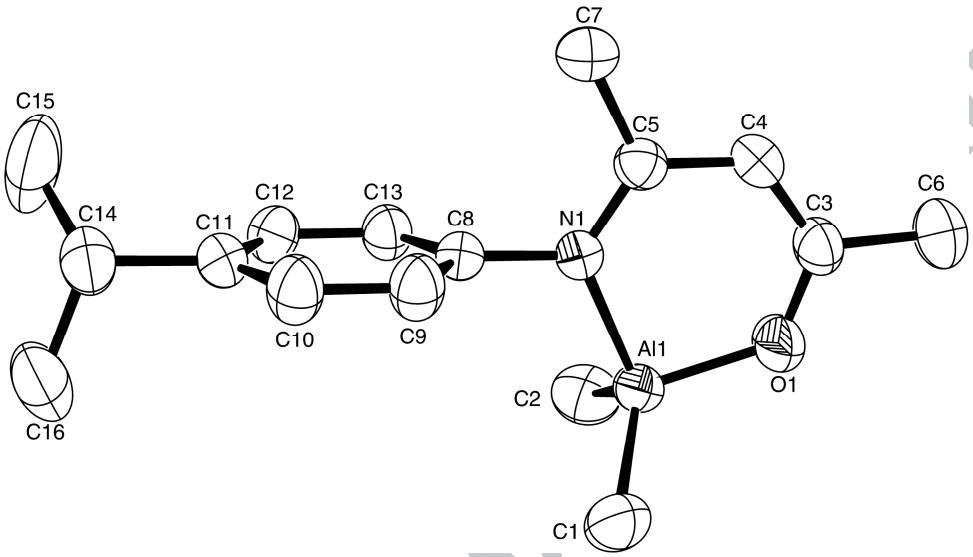

Fig. 4. Molecular structure of complex **3**. Thermal ellipsoids are drawn at the 50% probability level. Hydrogen atoms except for H35 on carbon atoms are omitted for clarity. Selected bond lengths [Å] and bond angles [°]: Al1–O1 1.8764(10), Al1–O2 1.8321(9), Al1–O3 1.8488(9), Al1–N1 2.0403(11), Al1–N2 2.0524(11), Al1–N3 2.0671(11), N1–C4 1.3232(16), N1–C6 1.4388(15), N2–C18 1.3151(15), N2–C20 1.4375(16), N3–C32 1.3189(16), N3–C34 1.4409(15), O1–C2 1.2933(16), O2–C16 1.2939(15), O3–C30 1.2821(16), O2–Al1–O3 178.80(5), O2–Al1–O1 93.71(4), O3–Al1–O1 87.34(4), O2–Al1–N1 89.74(4), O3–Al1–N1 90.90(4), O1–Al1–N1 87.98(4), O2–Al1–N2 89.91(4), O3–Al1–N2 89.50(4), O1–Al1–N2 89.32(4), N1–Al1–N2 177.25(5), O2–Al1–N3 91.91(4), O3–Al1–N3 87.06(4), O1–Al1–N3 174.32(4), N1–Al1–N3 91.21(4), N2–Al1–N3 91.52(4).

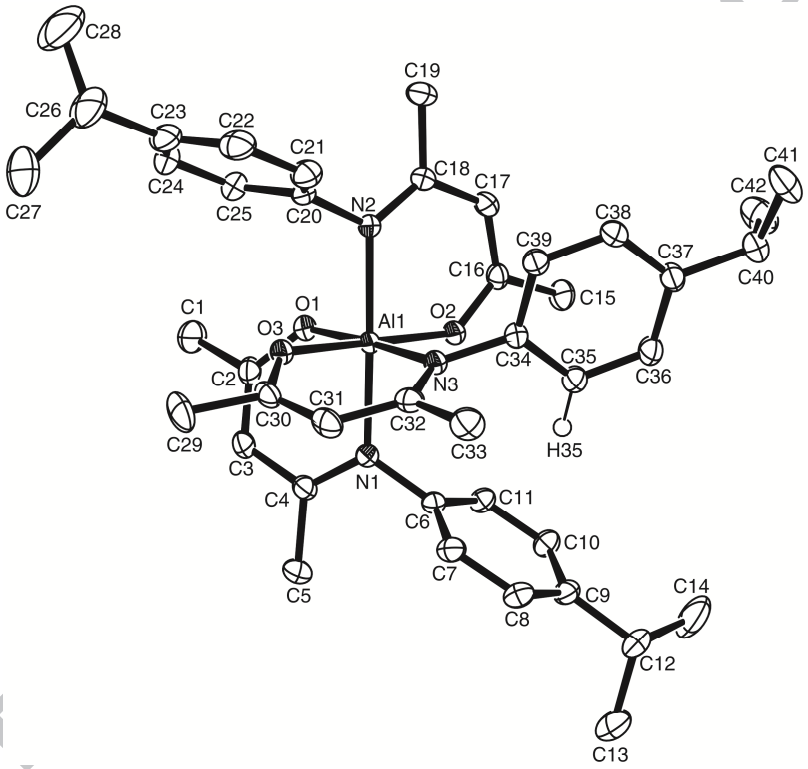

Fig. 5. Molecular structure of complex **6d.** Thermal ellipsoids are drawn at the 30% probability level. For clarity, hydrogen atoms are omitted and only selected atoms are labeled. Selected bond lengths [Å] and bond angles [°]: Al1−O1 1.8255(19), Al1−O2 1.9231(19), Al1−N1 2.080(2), Al1−Al2 2.8907(17), Al2−O3 1.695(2), Al2−O2 1.791(2), O1−Al1−O1* 98.90(13), O1−Al1−O2 167.81(9), O1−Al1−O2 93.27(8), O2−Al1−O2 74.58(11), O1−Al1−N1 83.72(9), O1−Al1−N1 88.80(8), O2−Al1−N1 95.83(9), O2−Al1−N1 93.33(8), O1−Al1−N1 83.72(9), N1−Al1−N1 168.48(13), O1−Al1−Al2 130.55(7), O2−Al1−Al2 37.29(6), Al2−O2−Al1 102.14(9), O3−Al2−O3* 116.67(18), O3−Al2−O2 108.80(10), O3−Al2−O2 118.38(11), O3−Al2−O2 118.38(11) , O3−Al2−O2 108.80(10), O2 −Al2 −O2* 81.14(12).

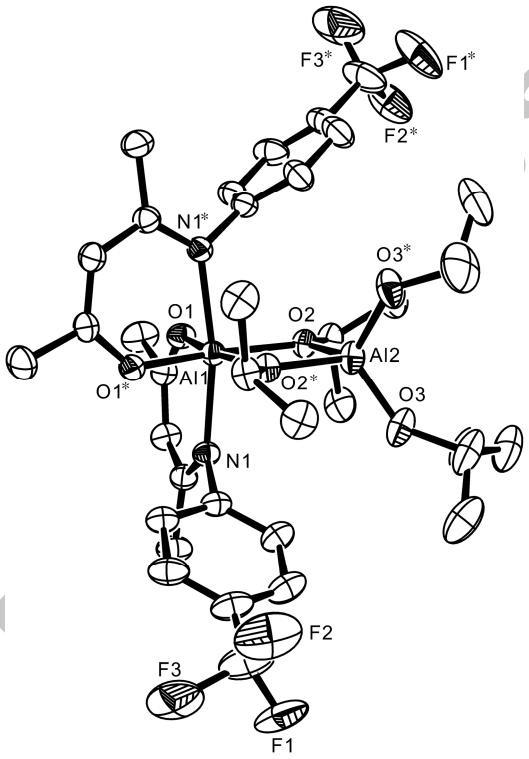

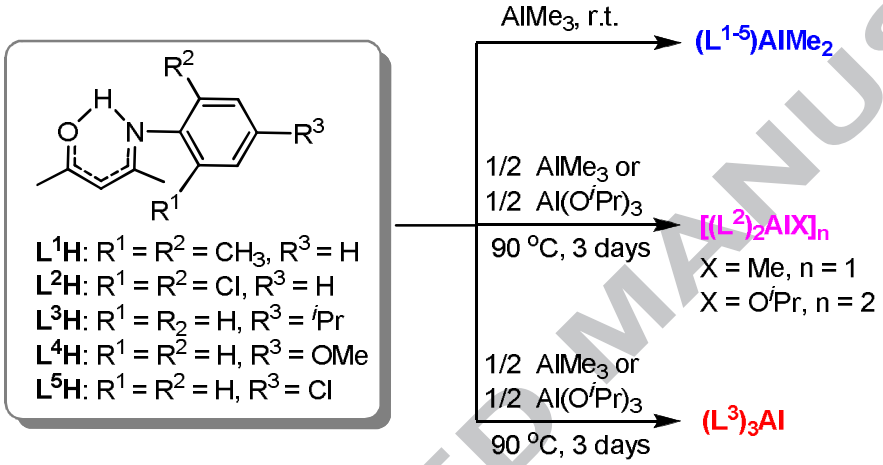

*Graphical Abstract - Synopsis

Aluminum Methyl and Isopropoxide Complexes with Ketiminate Ligands: Synthesis, Structural Characterization and Ring-Opening Polymerization of Cyclic Esters

Cigdem Tuc Altaf, Haobing Wang, Maryam Keram, Yang Yang and Haiyan Ma*

Several aluminum methyl and isopropoxide complexes bearing ketiminate ligands were synthesized, and characterized in selected cases with X-ray diffraction studies. These aluminum complexes proved to be active initiators for the ROP of *rac*-lactide and ε-caprolactone, affording polymers with high molecular weighs and broad distributions. Moderate isoselectivities were also achieved in the ROP of *rac*-lactide.